Silicon-29 Nuclear Magnetic Resonance Study of Silica

S. Lêonardelli,* L. Facchini, C. Fretigny, P. Tougne, and A. P. Legrand

Contribution from the Laboratoire de Physique Quantique, URA 421, E.S.P.C.I. 10 rue Vauquelin, 75231 Paris Cedex 05, France. *Received December 19, 1991*

Abstract: A ^{29}Si NMR study was carried out on different amorphous silica, using magic-angle spinning and proton decoupling with and without cross polarization, to obtain the surface concentration of hydroxyl groups. The samples were prepared at various stages of dehydration and with different methods of rehydration. It was found that the fraction of geminal hydroxyl silanol sites for all these samples is constant within the confidence limits of the accuracy of our data, and this indicates an equilibrium in the distribution of the hydroxyl groups at the silica surface.

Introduction

1. The Chemistry of Silica. The properties of amorphous silica of high specific surface area, from the smallest colloidal particles to macroscopic gels, depend largely on the chemistry of the surface in the solid phase. This is of practical importance in the technology of cracking catalysts, mineral processing, ceramics, and adsorbents.

An atom at the surface of a solid is only partially saturated and therefore possesses "residual valences" which are responsible for the adsorption of foreign atoms or molecules on the surface. In the case of silica, surface silicon atoms are bonded to one or more hydroxyl groups giving silanol sites. Since organic molecules can be adsorbed on siloxane or react with the silanol surface, the number and the kind of surface hydroxyl groups will determine the physicochemistry properties of these materials.

Silica can contain micropores into which water but not nitrogen—the adsorbate most commonly used to measure the surface area—can penetrate. So, since the area in micropores is difficult to define, the "surface" will generally be understood to mean that which is measured by the usual BET method of nitogen adsorption.[1]

As in silicate–water glass solutions studied by Marsmann,[2] the silica surface chemical species can be separated into the following groups[3]: $Si(O_{0.5})_4$, the siloxane groups Q^4 which form the bulk of the material; $Si(O_{0.5})_3OH$, the single hydroxyl silanol groups Q^3; and $Si(O_{0.5})_2(OH)_2$, the geminal hydroxyl silanol groups Q^2.

2. High-Temperature Treatment (HTT). To determine the number of surface hydroxyl groups, we must distinguish them from the physisorbed water, i.e. hydrogen-bonded water. This water can be removed from the outer surface with drying at 120 °C assuming that no micropores are present. In this case, silica can retain adsorbed water up to 180 °C.[4]

As silica samples are subjected to high temperature under vacuum, hydroxyl groups condense to form siloxane bonds and water is evolved. The rehydration of an anhydrous surface will be quickly followed by the adsorption of water molecules on the newly formed silanol surface. Also, when dehydration has been completed at temperatures higher than 800 °C, rehydration of such a surface can still proceed and is predisposed by the presence of nucleation sites which rarefy at high temperature.[5]

Since both dehydration and rehydration processes reflect basic underlying features of the organization of hydroxyl sites on the silica surface, the study of such phenomenon plays a central role in the description of surface structure. So, in order to characterize the samples studied in this report, we used both processes to obtain the number of hydroxyl groups per area unit as a function of thermal treatment, this being the most efficient method for modifying the chemical properties of the silica.

3. Techniques. Several techniques are used to study the number of hydroxyl groups. IR spectroscopy is a powerfull technique because it is possible to separate clearly OH groups from physisorbed water, but unfortunately the distinction between Q^2 and Q^3 sites is not obvious. One can also study the hydroxyl sites using silylation as a probe,[6] but since the geminal hydroxyl silanol sites can only chemically adsorb one molecule, when the single/geminal hydroxyl silanol ratio is unknown one cannot deduce the number of OH groups on the surface. On the other hand, it is not certain that the reaction is complete at the temperature of the experiment, so only the relative evolution of the number of OH groups on the surface as a function of temperature treatment can be deduced. Nuclear magnetic resonance (NMR) spectroscopy is sensitive to chemical environments of the silicon atom and does not suffer the objections given above.

The application of solid-state ^{29}Si NMR techniques with cross polarization and variable contact time experiments[7-11] to silica surfaces has provided new structural details on these materials, and the main result was the evidence of Q^2 sites and the quantitative evaluation of Q^4, Q^3, and Q^2 species.

The present paper deals with two complementary ^{29}Si NMR experiments combining magic-angle spinning (MAS) with high dipolar decoupling of protons with and without cross polarization (CP), respectively CP/MAS and ^1H DEC/MAS NMR experiments. The concentrations of the different species on the silica surface can be obtained by quantitative analysis of the spectra arising from experiments of this type.[12]

Experimental Section

1. Silica. The samples are amorphous silica powder with high specific area that can be grouped into two categories. (1) Silica obtained by different synthesis processes: (a) silica Aerosil from Degussa A200 obtained by high-temperature hydrolysis of $SiCl_4$ gas in a flame of hydrogen and air at about 1000 °C with a specific area, determined by nitrogen adsorption at 77 K (BET), of 215 m^2/g; (b) precipitated silica Z175 MP, obtained by the action of sulfuric acid on an aqueous sodium silicate with a specific area of 201 m^2/g (BET); and (c) silica gel (S) prepared by the action of sulfamic acid on a magnesium silicate with a specific area of 460 m^2/g (BET). (2) Silica prepared by different treatments of the reference silica Z175 MP: (a) the first series of samples Z175 C and Z175 D results from thermal treatments (respectively at 600 and 700 °C (with nitrogen) lasting 6 h of Z175 MP dried at 120 °C; (b) the second series of samples results from different thermal treatments under dynamic vacuum of the Z150 silica obtained by heating the reference silica for 1.5 h at 150 °C—Z300, Z400, Z500, Z600, and Z700 samples correspond to thermal treatments lasting 6 h of Z150 respectively

(1) Iler, R. K. *The Chemistry of Silica*; John Wiley & Sons: New York, 1979; pp 625.
(2) Marsmann, H. C. *Z. Naturforsch.* **1974**, *29b*, 495–499.
(3) Englehardt, G.; Jancke, H.; Hoebbel, D.; Wiecker, W. *Z. Chem.* **1974**, *14*, 109–110.
(4) Iler, R. K. *The Chemistry of Silica*; John Wiley & Sons: New York, 1979; pp 629.
(5) Dietz, N. R.; Turner, N. H. *J. Phys. Chem.* **1971**, *75*, 2718–2727.
(6) Sindorf, D. W.; Maciel, G. E. *J. Phys. Chem.* **1982**, *86*, 5208–5219.
(7) Maciel, G. E.; Sindorf, D. W. *J. Am. Chem. Soc.* **1980**, *102*, 7606–7607.
(8) Lippmaa, E.; Samoson, A.; Brej, V.; Gorlov, Ju. *Dokl. Akad. Nauk SSSR* **1981**, *259*, 403–408.
(9) Grimmer, A. R.; Starke, P.; Wieker, W.; Mägi, M. *Z. Chem.* **1982**, *22*, 44.
(10) Grimmer, A. R.; Starke, P.; Mägi, M. *Z. Chem.* **1986**, *26*, 114–115.
(11) Starke, P.; Trettin, R.; Grimmer, A. R. *Z. Chem.* **1986**, *26*, 114.
(12) Grimmer, A. R.; Rosenberger, R.; Bürger, H.; Vogel, W. *J. Non-Cryst. Solids* **1988**, *99*, 371–378.

0002-7863/92/1514-6412$03.00/0

at 300, 400, 500, 600, and 700 °C after which all samples were placed in an enclosure at 20 °C under saturated water vapor for 24 h; and (c) silica Z175 B5 was obtained by heating the reference silica under air for 6 h at 500 °C.

2. NMR Measurements. The solid-state ^{29}Si NMR measurements were performed on a Bruker CXP 300 spectrometer at 59.6 MHz. Magic-angle spinning was routinely carried out at a 4 kHz spinning rate in a double bearing probe head. Optimization of the Hartmann–Hahn condition and the magic angle were obtained with the standard Q_8M_8 sample.[13,14] The spectra of the silica samples were typically recorded by using a repetition time of 2–4 s for cross-polarization experiments and 120 s without cross-polarization experiments (240 s for Aerosil). The duration time for obtaining the 90° pulse was 4–5 μs. The number of scans ranged from 1000 to 5000 for CP/MAS experiments and from 100 to 150 without CP.

Results and Interpretation

1. ^{29}Si NMR Features. Figure 1 shows the structural resolution obtainable in ^{29}Si NMR MAS and ^1H decoupling spectra of a precipitated silica (Z175 MP) and of a silica gel (S) in the most favorable cases and their decomposition into three components using an appropriate fit procedure. The isotropic ^{29}Si chemical shifts of the three signals are about −91, −101, and −110 ppm and respectively reflect the presence of Q^2, Q^3, and Q^4 units. Chemical shifts are given with respect to the most intense silicon resonance in Q_8M_8 (11.6 ppm/TMS). Without cross polarization, all the silicons are observed (bulk experiment) and the concentrations of Q^2, Q^3, and Q^4 species can be deduced, using a curve-fitting program. Unfortunately the experiments are very long because of the long spin–lattice relaxation time of ^{29}Si (repetition time must be about 120–240 s), and because of the small number of geminal hydroxyl groups, the precision of the fit can be very poor. So only the fraction of silanol sites (geminal and single) in the material (ratio f_s) can be obtained with good precision.[15]

With cross polarization (Figure 2), the whole siloxane group is not observed (because the proton is too far from these silicon sites) and only the fraction of geminal hydroxyl silanol sites (ratio f_g) can be deduced from the evolution of the spectra versus contact time.[16] Combining the results of both experiments with and without cross polarization allows the determination of the concentrations of Q^2, Q^3, and Q^4 sites.

To obtain better fits, data of ^1H DEC/MAS spectra (1500 points per spectrum) were transferred to an IBM PC computer. Synthetic spectra were generated using a function consisting of three overlapping Gaussian lines (decomposition in two components led to similar results). The nine associated variables (width, area, and chemical shift for each of the three peaks) were adjusted to minimize the root-mean-square error between the observed and calculated spectrum using a method of nonlinear regression.

For better resolved CP/MAS spectra, the line-shape analysis was obtained using the Bruker visual curve-fitting program LINFIT with the Aspect 2000 calculator. This program gives the position, width, relative intensity, and area of each line. Final evaluation of relative peak area versus contact time gives best results with constraint on the three resonance positions and widths. In this way we obtain the fraction of area of each Q^i group in each total simulated spectrum and then multiply this relative peak area by the total area of the real spectrum to reflect the evolution of the spectra as a function of contact time. The evolution of the magnetization (simulated area) for the three lines as a function of contact time τ in CP/MAS experiments can be fitted by the classical law[17,18]

$$M_i(\tau) = M_{0i}\,\lambda^{-1}(1 - \exp(-\lambda\tau/T_{SiH}{}^i))\,\exp(-\tau/T_{1\rho}^{H,i})$$

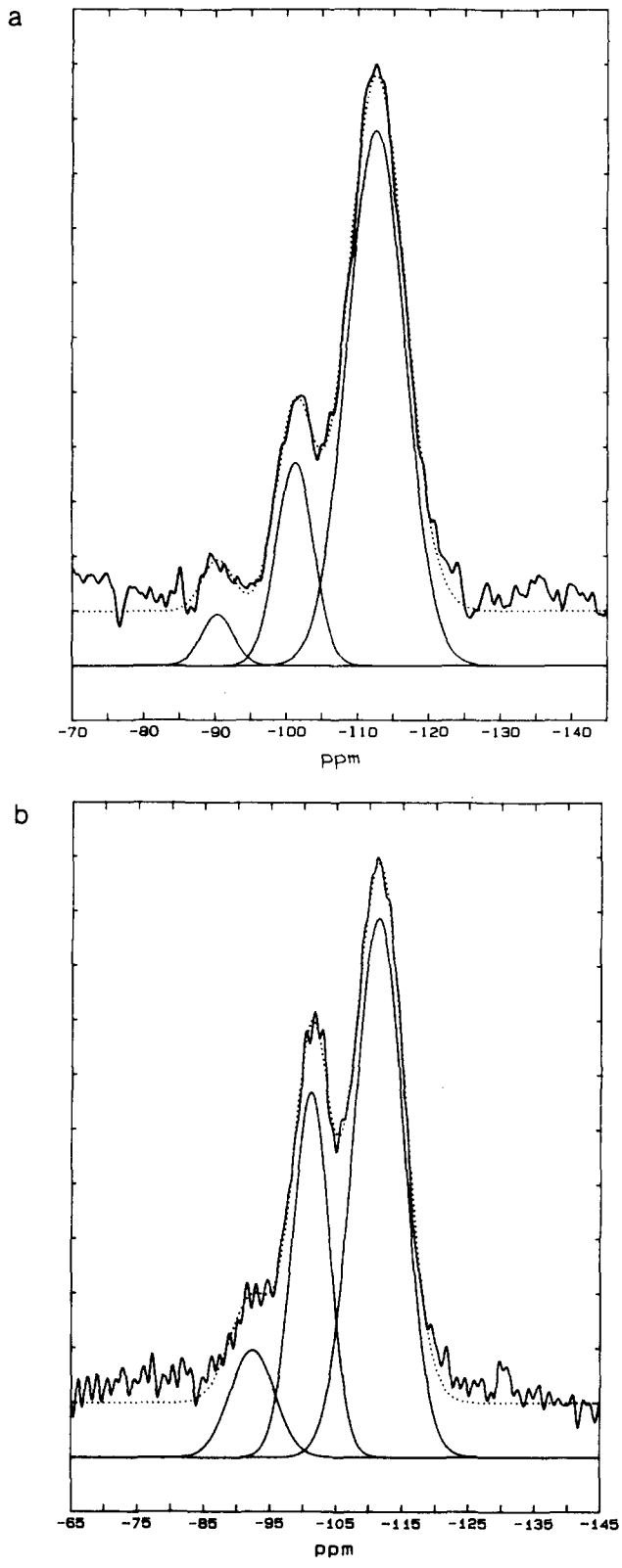

Figure 1. 59.6-MHz ^{29}Si ^1H DEC/MAS NMR spectrum of Z175 MP silica (a) and silica gel (S) (b). Examples of the application of the curve-fitting program applied to these spectra. Experimental conditions: number of scans 100–150; repetition time 120 s.

with $\lambda \simeq 1 - T_{SiH}{}^i/T_{1\rho}^{H,i}$ assuming that $T_{1\rho}^{Si,i} \gg T_{SiH}{}^i$ (which is justified for all the samples we studied here, see Table II). The index i corresponds to the superscript of the Q^i group and M_{0i} is the limit aimantation which is proportional to the number of silicons of the Q^i group. $T_{1\rho}^H$ and T_{SiH} are respectively the proton spin–lattice relaxation time in the rotating frame and the silicon–proton cross-polarization time. The parameters M_0, $T_{1\rho}^H$, and

(13) Lippmaa, E.; Samoson, A. *Brücker Rep.* **1982**, *1*, 6–9.
(14) Engelhardt, G.; Michel, D. *High Resolution Solid State NMR of Silicates and Zeolites*; John Wiley & Sons: New York, 1987; pp 113–114.
(15) Legrand, A. P.; Hommel, H.; Taïbi, H.; Miquel, J. L.; Tougne, P. *Colloids Surf.* **1990**, *45*, 391–411.
(16) Sindorf, D. W.; Maciel, G. E. *J. Am. Chem. Soc.* **1983**, *105*, 1487–1493.
(17) Pines, A.; Gibby, M. G.; Waugh, J. S. *J. Chem. Phys.* **1973**, *59*, 569–589.
(18) Mehring, M. *Principles of High Resolution NMR in Solids*; Springer-Verlag: Berlin, Heidelberg, New York, 1983; pp 143–155.

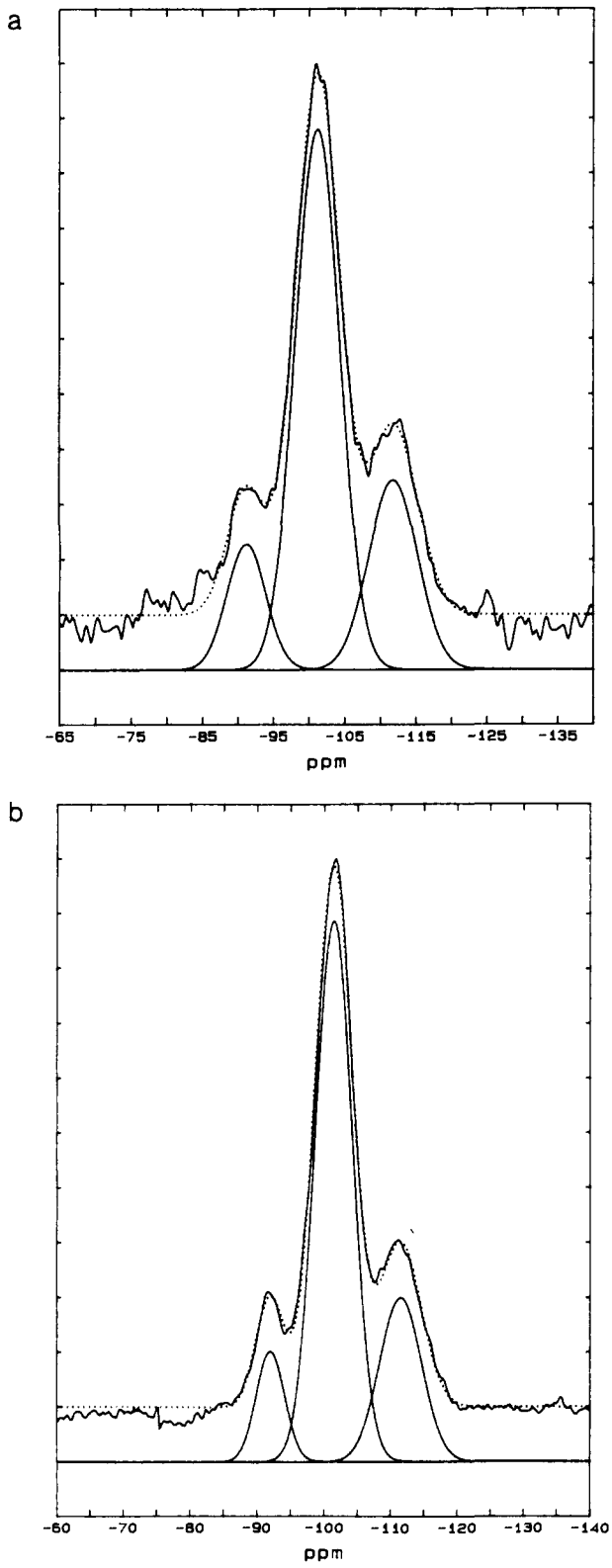

Figure 2. 59.6-MHz ^{29}Si CP/MAS NMR spectra of Z175 MP silica (a) and silica gel (S) (b). Examples of the application of the LINFIT curve-fitting program to these spectra. Experimental conditions: (a) cross polarization time (t_{cp}) = 3.5 ms, number of scans (n_s) = 1100, repetition time (t) = 2 s; (b) t_{cp} = 4.5 ms; n_s = 900; t = 2 s.

T_{SiH} for each silicon of a given type are obtained by least-squares fitting of the formula (Figure 3). Within our experimental error, we do not observed the oscillatory component of the magnetization transfer as in the paper by Walther et al.[19]

(19) Walther, K. L.; Wokaun, A.; Baiker, A. *Mol. Phys.* **1990**, *71*, 769–780.

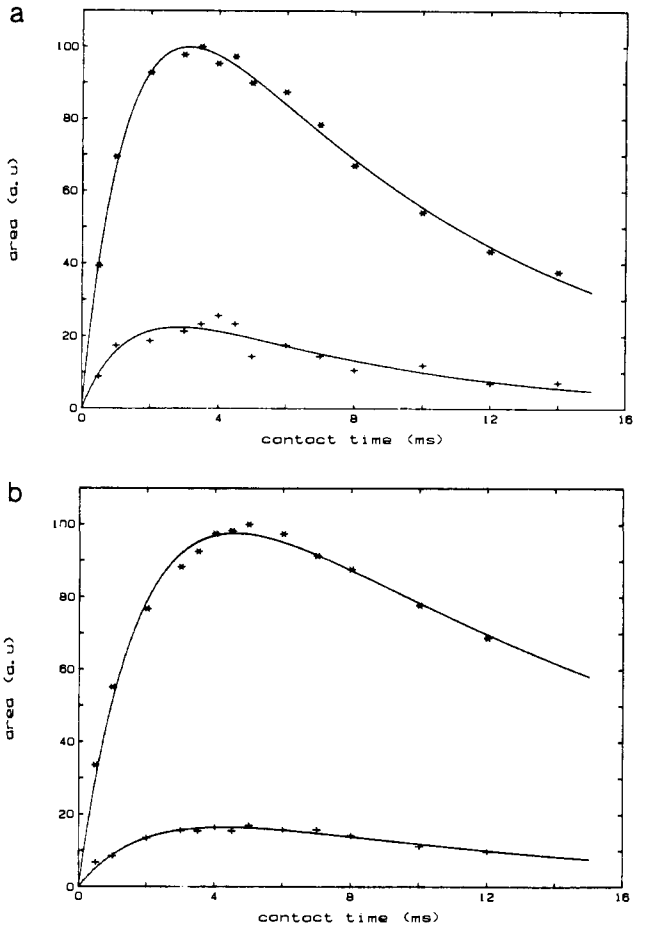

Figure 3. Plot of the magnetization versus contact time for Z175 MP (a) and silica gel (S) (b) samples: (*) data obtained for single hydroxyl silanol sites and (+) data obtained for geminal hydroxyl silanol sites.

Positions and widths of the simulated lines and parameter values are reported in Tables I and II. The exclusion of the resonance at −110 ppm associated with Q^4 sites is intentional, since unfavorable relaxation properties (long T_{SiH} values) make this peak generally unsuitable for quantitative interpretations.

To summarize, from CP/MAS experiments we deduce the fractional population of surface geminal hydroxyl silanol sites

$$f_g = \frac{M_{02}}{M_{02} + M_{03}}$$

and ^1H DEC/MAS experiments give the fractional population of silanol sites

$$f_s = \frac{I_2 + I_3}{I_2 + I_3 + I_4}$$

where I_i is the simulated peak area of the Q^i group.

2. Composition of the Silica. If we define the proportions of the different chemical species in the material Q^4, Q^3, and Q^2 respectively as z, y, and x, we obtain the general formula of the silica

$$(SiO_2)_z(SiO_{5/2}H)_y(SiO_3H_2)_x$$

with $x + y + z = 1$, a global formula being

$$SiO_2(H_2O)_{0.5(y+2x)}$$

This presentation is interesting because we understand naturally how the number of OH groups can be deduced from the general loss in weight corresponding to the evolution of the molecular water from silica samples subjected to high-temperature treatment under vacuum.

The two types of experiments we performed allowed us to obtain the following: $f_g = x/(x + y)$ and $f_s = x + y$. And with the

Table I. Chemical Shifts and Widths of the Simulated Lines

		CP/MAS spectra		MAS/DEC ^1H spectra	
silica		chemical shift (ppm)	width (Hz)	chemical shift (ppm)	width (Hz)
A200	geminal	−91.2	331	−89.8	354 ± 35
	single	−100.5	465	−99.3	537 ± 30
	siloxane	−110.4	525	−110.5	646 ± 15
Z175 MP	geminal	−91.2	386	−90.5	315 ± 25
	single	−101.2	437	−101.2	368 ± 10
	siloxane	−111.8	484	−112.6	568 ± 05
Z175 B5	geminal	−91.8	416	−90.1	536 ± 75
	single	−101.0	456	−100.3	467 ± 15
	siloxane	−110.5	606	−111.1	683 ± 05
Z175 C	geminal	−91.0	380	−91.0	663 ± 160
	single	−100.2	462	−99.9	411 ± 20
	siloxane	−109.9	668	−111.1	750 ± 10
Z175 D	geminal	−91.5	396	−90.8	211 ± 40
	single	−100.6	454	−100.0	532 ± 40
	siloxane	−110.3	669	−111.5	736 ± 10
Gel S	geminal	−92.0	297	−92.5	469 ± 30
	single	−101.5	389	−101.2	389 ± 05
	siloxane	−111.5	443	−111.4	524 ± 05
Z150	geminal	−92.0	396	−92.1	353 ± 45
	single	−101.5	403	−101.0	440 ± 15
	siloxane	−111.7	489	−111.6	523 ± 05
Z300	geminal	−91.5	378	−92.3	377 ± 30
	single	−101.3	432	−101.6	462 ± 20
	siloxane	−111.7	516	−112.1	581 ± 05
Z400	geminal	−91.0	428	−91.1	304 ± 20
	single	−101.0	473	−100.7	447 ± 15
	siloxane	−111.3	556	−111.9	630 ± 05
Z500	geminal	−91.4	377	−91.5	477 ± 50
	single	−100.5	449	−100.0	421 ± 20
	siloxane	−110.3	642	−110.7	644 ± 05
Z600	geminal	−91.5	396	−90.1	352 ± 20
	single	−100.7	478	−99.6	461 ± 15
	siloxane	−110.9	567	−110.6	708 ± 05
Z700	geminal	−90.9	365	−92.0	433 ± 40
	single	−100.3	484	−98.9	547 ± 40
	siloxane	−110.1	625	−110.1	805 ± 10

knowledge that $x + y + z = 1$, we can calculate the values of the concentrations x, y, and z (Table III) given by

$$x = f_g f_s \qquad y = f_s(1 - f_g) \qquad z = 1 - f_s$$

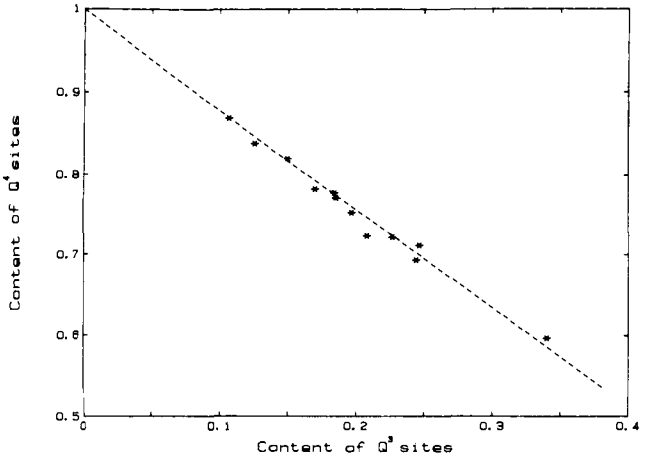

Figure 4. Plot of the content of siloxane sites versus the content of single hydroxyl silanol sites for all samples studied.

Now it is possible to correlate the number of OH groups per unit area to the molar number of OH groups $2x + y$ with the assumption that all the hydroxyl groups are on the outer surface, i.e. on the surface measured by the BET method. If n_{OH} is the number of OH groups per square nanometer, d the number of silicon atoms per gram of compound, and S the specific area (nm^2/g), we have the relation

$$(y + 2x)d = n_{OH}S = f_s(1 + f_g)d$$

The molecular weight of the silica also depends on $2x + y$ as follows

$$M(x) = 60.06 + 9(2x + y) \simeq 60 + 9f_s(1 + f_g)$$

with $d = N_A/M$ (N_A is the Avogadro number), n_{OH} is given by

$$n_{OH} = \frac{f_s(1 + f_g)}{S} \frac{N_A}{60 + 9f_s(1 + f_g)}$$

n_{OH} values (Table IV) for each of the samples studied here have been calculated using the BET specific area. Studies of nitrogen adsorption isotherms at 77 K on Aerosil and Z175 MP subjected to different temperatures for 16 h under vacuum have shown that BET areas determined this way remain essentially constant between 25 and 650 °C for these two samples.[20] Moreover, the

Table II. Values of the Parameters[a] Obtained from Analysis of CP/MAS Experiments

silica	silanol	M_0 (au)	Δ_R[b] (%)	$T_{1\rho}^H$ (ms)	Δ_R[b] (%)	T_{SiH} (ms)	Δ_R[b] (%)
A200	geminal	26.0 ± 1.5	5.6	19.0 ± 3.5	18.6	0.9 ± 0.1	16
	single	124.9 ± 7.1	5.7	15.0 ± 1.9	12.4	1.6 ± 0.2	12
Z175 MP	geminal	33.7 ± 5.3	15.7	6.9 ± 1.8	26.1	1.4 ± 0.4	30
	single	140.9 ± 3.5	2.5	9.1 ± 0.4	4.8	1.4 ± 0.1	5
Z175 B5	geminal	21.7 ± 1.3	6.0	17.6 ± 2.8	16.1	0.6 ± 0.1	20
	single	103.1 ± 4.0	3.9	32.6 ± 5.4	16.5	0.7 ± 0.1	13
Z175 C	geminal	34.5 ± 1.2	3.4	10.8 ± 1.1	10.5	0.9 ± 0.1	12
	single	120.0 ± 5.5	4.6	13.1 ± 1.1	8.7	0.9 ± 0.1	9
Z175 D	geminal	18.0 ± 1.7	9.5	23.9 ± 7.0	29.4	0.4 ± 0.2	43
	single	80.9 ± 2.8	3.5	35.2 ± 5.0	14.2	0.4 ± 0.1	15
Gel S	geminal	24.3 ± 2.5	10.2	11.0 ± 2.3	20.8	2.1 ± 0.4	17
	single	129.2 ± 5.7	4.4	16.3 ± 2.0	12.4	1.9 ± 0.2	8
Z150	geminal	25.3 ± 2.0	7.8	8.4 ± 1.2	14.2	1.4 ± 0.2	15
	single	148.1 ± 5.6	3.8	10.3 ± 0.7	7.1	2.0 ± 0.1	6
Z300	geminal	27.8 ± 2.8	10.2	10.2 ± 2.1	20.0	1.5 ± 0.3	20
	single	120.1 ± 4.8	4.0	21.2 ± 2.7	12.8	1.4 ± 0.1	9
Z400	geminal	32.9 ± 3.3	10.1	10.4 ± 2.1	20.3	1.3 ± 0.3	26
	single	116.1 ± 4.4	3.8	22.4 ± 2.9	12.8	1.2 ± 0.1	11
Z500	geminal	29.4 ± 2.3	7.7	18.7 ± 4.2	22.6	1.3 ± 0.2	18
	single	87.5 ± 2.8	3.2	42.6 ± 8.4	19.8	0.6 ± 0.1	13
Z600	geminal	38.7 ± 5.5	14.2	7.7 ± 1.6	20.8	2.6 ± 0.5	29
	single	147.2 ± 7.1	4.8	11.1 ± 1.0	8.9	2.3 ± 0.2	7
Z700	geminal	30.3 ± 6.5	21.4	8.3 ± 2.7	32.7	2.6 ± 0.8	30
	single	150.3 ± 17.0	11.3	11.4 ± 2.3	19.9	3.6 ± 0.5	14

[a] M_0 is the limit aimantation, $T_{1\rho}^H$ is the proton spin–lattice relaxation time in the rotating frame, and T_{SiH} is the cross-polarization time. [b] Δ_R is the relative error upon the previous value in the column.

Table III. Contents of Q^2 (x), Q^3 (y), and Q^4 (z) Sites

silica	f_g (%)	f_s (%)	x (%)	y (%)	z (%)
A200	17.2 ± 1.9	30.7 ± 3.4	5.3 ± 1.2	24.4 ± 2.1	69.3 ± 4.1
Z175 MP	19.3 ± 4.0	23.0 ± 0.9	4.4 ± 1.1	18.5 ± 0.2	77.0 ± 1.4
Z175 B5	17.4 ± 1.8	22.3 ± 2.0	3.9 ± 0.7	18.4 ± 1.3	77.7 ± 2.3
Z175 C	22.3 ± 1.7	16.2 ± 2.4	3.6 ± 0.8	12.6 ± 1.6	83.8 ± 3.3
Z175 D	18.2 ± 2.6	13.1 ± 1.8	2.4 ± 0.7	10.7 ± 1.1	86.9 ± 3.4
Gel S	15.8 ± 2.5	40.4 ± 1.8	6.4 ± 1.3	34.0 ± 0.5	59.6 ± 1.4
Z150	14.6 ± 1.8	28.9 ± 2.0	4.2 ± 0.8	24.7 ± 1.2	71.1 ± 2.0
Z300	18.8 ± 2.9	27.9 ± 2.0	5.2 ± 1.2	22.7 ± 0.9	72.1 ± 2.3
Z400	22.1 ± 3.4	21.8 ± 1.1	4.8 ± 1.0	17.0 ± 0.1	78.2 ± 1.6
Z500	24.6 ± 2.7	27.7 ± 2.9	7.0 ± 1.6	20.8 ± 1.3	72.3 ± 2.6
Z600	20.8 ± 4.4	24.9 ± 1.5	5.2 ± 1.4	19.7 ± 0.1	75.1 ± 2.0
Z700	16.8 ± 5.8	18.0 ± 2.7	3.0 ± 1.5	15.0 ± 1.2	82.0 ± 4.1

Table IV. Calculated and Estimated Number of Hydroxyl Groups per Unit Area in the Different Samples

silica	S_{BET} (m^2/g)	n_{OH} (OH/nm^2)	n_{OH}^t (OH/nm^2)
A200	215	15.9 ± 2.1	16.9
Z175 MP	201	13.1 ± 1.0	13.5
Z175 B5	201	12.6 ± 1.4	13.1
Z175 C	201	9.6 ± 1.6	9.5
Z175 D	201	7.6 ± 1.2	7.7
Gel S	460	9.5 ± 0.7	10.4
Z150	201	15.7 ± 1.4	17.0
Z300	201	15.8 ± 1.6	16.4
Z400	201	12.8 ± 1.0	12.9
Z500	201	16.4 ± 2.2	16.3
Z600	201	14.4 ± 1.5	14.7
Z700	201	10.2 ± 2.1	10.6

BET method gives the same results for hydroxylated or dehydrated surfaces.[21] Therefore we take 201 m^2/g as the specific area for all samples resulting from the treatment of Z175 MP.

3. Notes About the Experimental and Fitting Error. It is very difficult to define an error bar on x, y, and z after the different steps of our analysis. The contributions to the error bar can be listed as follows: (a) experimental error caused by the NMR spectrometer during the acquisition time (noise, dead time); (b) curve-fitting error caused by simulation with three Gaussian curves on the spectra obtained with MAS and decoupling of the protons; and (c) curve-fitting error for the evolution of the magnetization as a function of contact time. Error bars reported here reflect only the general reproducibility of the fitting procedures used in evaluating the ratios f_g and f_s and thus can be considered as rough confidence limits of the accuracy of these data.

Discussion

1. Dehydration/Rehydration Experiments. Let us note the evolution of the relaxation times as a function of the high-temperature treatment. We will not discuss here the cause of this evolution (we must study in more detail the influence of physisorbed water), but we observe that the conditions have greatly changed with the high-temperature treatment (HTT). For this reason it would have been very ambiguous to analyze the cross-polarization spectra with only one measurement at a fixed contact time for different HTT. Increasing temperature causes a significant increase of the line width of the Q^4 units. This line width is mainly affected by the dispersion of isotropic chemical shifts due to structural disorder. Therefore, since different environments of a silicon site are created by the distorsion of bond angles and bond lengths,[22] the width distribution of the Si–O–Si angle for Q^4 units increases with increasing temperature. We also notice that the line widths of siloxane lines are generally greater in ^1H DEC/MAS experiments than in CP/MAS experiments. This effect can arise from the chemical shift differences between surface and bulk siloxanes in connection with strained and unstrained rings.[23]

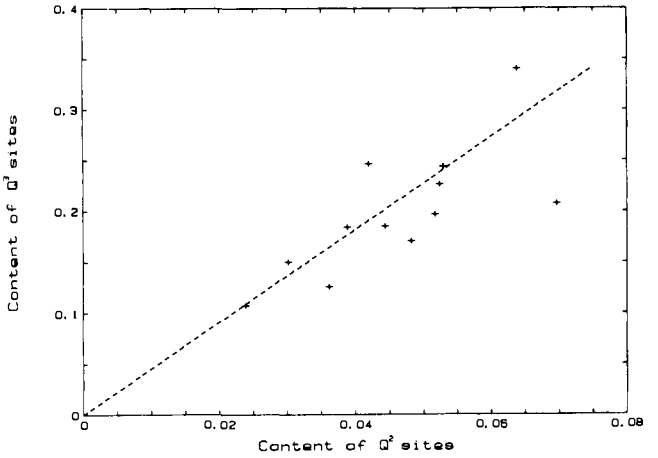

Figure 5. Plot of the content of single hydroxyl silanol sites versus the content of geminal hydroxyl silanol sites for all samples studied.

With the two kinds of experiments we performed, we have obtained the values of the concentrations x, y, and z. We can observe that Q^2 sites (x) are always present at each temperature of our experiment. Several papers have presented studies on the evolution of geminal hydroxyl sites as a function of dehydration temperature. On a silica gel glass dried and fired in the 200–900 °C range, Grimmer et al.[12] observed by ^{29}Si CP/MAS NMR a small amount of Q^2 sites at each temperature. On Aerosil silicas dehydrated under vacuum at different temperatures, Morrow et al.[24] showed that geminal hydroxyl silanol sites observed by CP/MAS do persist on silica even after evacuation at 800 °C. On amorphous silica gels after heat treatments between 50 and 1100 °C, Brinker et al.[25] observed that geminal hydroxyl silanol groups are still present after activation at 1100 °C.

If we now report the evolutions of x, y, and z as a function of HTT in the graph $z = f(y)$ or $y = f(x)$ (Figures 4 and 5) we can observe that the experimental points are distributed along a straight line:

$$z = 1 - \frac{1}{1-f_g}y = 1 - \beta y \text{ and } y = \frac{1-f_g}{f_g}x = \alpha x$$

$$\beta = 1.2 \text{ and } \alpha = 4.6$$

From these values, we can deduce that the average value of $f_g = x/x + y$ is

$$f_g = 1/\alpha\beta = 0.18$$

This result implies that within the confidence limits of the accuracy of our data, the fraction of silanol sites present as geminal

(20) Legrand, A. P. et al. *Advances in colloid and Interface science*; Elsevier Science Publishers: Amsterdam, 1990; pp 233–235.
(21) Iler, R. K. *The Chemistry of Silica*; John Wiley & Sons: New York, 1979; pp 466–468.
(22) Engelhardt, G.; Michel, D. *High Resolution Solid State NMR of Silicates and Zeolites*; John Wiley & Sons: New York, 1987; pp 117.
(23) Tuel, A.; Hommel, H.; Legrand, A. P.; Chevallier, Y.; Morawski, J. C. *J. Colloids Surf.* **1990**, *45*, 413–428.
(24) Morrow, B. A.; Gay, I. D. *J. Phys. Chem.* **1988**, *92*, 5569–5571.
(25) Brinker, C. J.; Kirkpatrick, R. J.; Tallant, D. R.; Bunker, B. C.; Montez, B. *J. Non-Cryst. Solids* **1988**, *99*, 418–428.

sites (f_g) remains essentially constant for amorphous silica prepared by different synthesis processes or obtained by different thermal treatment of a precipitated silica rehydrated naturally at room temperature or over 24 h at 20 °C under saturated vapor pressure. Therefore, we can suppose that this result could be generalized to all amorphous silica exposed to water whatever the treatment they undergone. Several papers have concluded that Q^2 sites are always present on different types of temperature-treated silica, and it seems possible that a proportionality (α) could exist between the number of single hydroxyl silanol sites and the number of geminal hydroxyl silanol sites in these samples. With the presence of water molecules, an equilibrium in the distribution of the silanol sites at the silica surface is established. Studies by IR spectroscopy have also revealed that there is no noticeable difference between single and geminal hydroxyl sites in their behavior when water molecules are adsorbed.[26] In fact, the distribution of the hydroxyl groups appears to be an intrinsic physicochemical constant of this kind of compound.

Since the molar number of geminal hydroxyl groups is $2x$, the fraction of geminal hydroxyl groups in the samples is given by

$$\% \mathrm{OH_g} = \frac{2x}{2x + y} = \frac{2f_g}{1 + f_g} = \frac{2}{\alpha + 2} \simeq 30\%$$

About 30% of the hydroxyl groups in amorphous silica are present as geminal hydroxyl groups. The remaining 70% could be single or vicinal hydroxyl groups that NMR cannot distinguish as IR spectroscopy can. This population of geminal hydroxyl sites has already been observed by several authors on a desactivated gel at 25 °C (Fisher S157).[16,27]

2. Concentration of Hydroxyl Groups. (a) Determination. With the previous result, we can obtain the general average formula of the silica

$$SiO_2(H_2O)_{3.3x}$$

Or with the most detailed formula

$$(SiO_2)_{1-5.5x}(SiO_{5/2}H)_{4.5x}(SiO_3H_2)_x$$

The relationship between x and n_{OH} becomes

$$x = \frac{1}{\alpha + 2}\frac{S}{N_A}Mn_{OH}$$

Expressing the molecular weight of the silica versus x, $M \simeq 60 + 9x(\alpha + 2)$, we deduce

$$x = \frac{60S}{N_A(\alpha + 2)}n_{OH}\frac{1}{1 - 9(S/N_A)n_{OH}}$$

With our usual value of $n_{OH} = 10$ OH/nm^2, $S = 200 \times 10^{18}$ nm^2/g, and $N_A \simeq 6 \times 10^{23}$, we can neglect the defect to the linearity of x versus n_{OH} because

$$9(S/N_A)n_{OH} \simeq 3\% \text{ and so } M \simeq 60 \text{ g}$$

So we obtain

$$x = \frac{S}{655}n_{OH}^{\,t} \qquad y = \frac{S}{144}n_{OH}^{\,t} \qquad n_{OH}^{\,t} = 1.18f_s\frac{100}{S}$$

where $n_{OH}^{\,t}$ is a theoretical value of n_{OH} in OH/nm^2 (Table IV) calculated with $f_g = 0.18$, x and y are expressed in percent, and S is in m^2/g.

With the previous expression we can obtain the concentration of OH groups in these silica using only one NMR experiment providing the value of the f_s parameter.

(b) Evolution. From the evolution of x or y as a function of HTT, we can deduce the evolution of n_{OH} versus HTT (Figure 6). The surface density of hydroxyl groups appears to be very sensitive to the rehydration mode. The mean value of the number of hydroxyl groups obtained after hydration over 24 h (at 20 °C and 100% humidity) is greater than the one obtained after hydration at room temperature and humidity. These data show that, at temperatures up to about 500 °C, most of the silanol groups removed by dehydration are restored following exposure to liquid water (except for the sample tempered at 400 °C which seems to have been incompletely rehydrated). At higher temperature, however, rehydration becomes increasingly inefficient because the silica surface becomes hydrophobic. Lowen and Broge[28] have already observed that the extent of rehydration on the surface depends on both the dehydration temperature of the silica and the relative hygrometric percentage used for this rehydration.

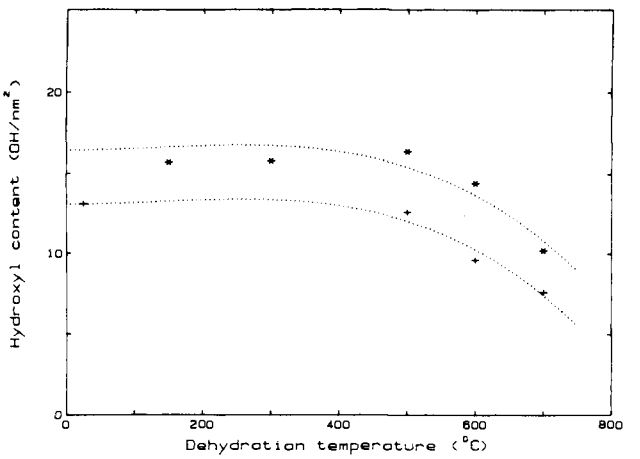

Figure 6. Concentration of surface hydroxyl groups versus dehydration temperature for silica samples prepared by treatment of the reference silica: (*) data obtained for silica samples rehydrated over 24 h (at 20 °C and 100% humidity); (+) data obtained for silica samples rehydrated at room temperature and humidity.

(c) Discussion. It is important to point out that the concentrations of surface hydroxyl groups we obtained, especially for Aerosil silica (but which are similar to other NMR results on this sample[19,23]), are greater than the ones generally reported with other techniques and than the theoretical values calculated on geometric considerations and the density of amorphous silica.[29] For example, after deuterium exchange and mass-spectrometric analysis of a large number of amorphous silica, Zhuravlev[30] shows that the surface density of OH groups is a physicochemical constant for the fully hydroxylated surface and that its average value after evacuation at 200 °C is 4.9 OH/nm^2. This surface concentration is obtained with respect to specific area determined by krypton adsorption using the BET method. In this case, the results are less affected by the nature of the surface than when nitrogen is used.

Two considerations can have great importance in the discussion about the number of hydroxyl groups reported in Table IV. First, the measure of the specific area by nitrogen adsorption can be less efficient when we desire to study the behavior of water molecules smaller than nitrogen molecules. Consequently, the specific area accessible to water could be underestimated, giving too high contents of hydroxyl groups. Secondly, NMR spectroscopy can determine higher numbers of hydroxyl groups than generally obtained using other techniques because it takes into account all the hydroxyl groups present in the sample, i.e. both surface hydroxyl groups and internal hydroxyl groups which are structural water or OH groups inside the silica particles and are inaccessible to small molecules such methanol or deuterium.

Conclusion

In summary, the constant value of f_g implies that the general behavior of the single and so geminal hydroxyl silanol sites follows that observed for the overall hydroxyl population. Therefore a chemical equilibrium which is independant of the total number of OH groups at the silica surface is established in these materials

(26) Sauer, J.; Schröder, K. P. *Z. Phys. Chem., Leipzig* **1985**, *266*, 379–387.
(27) Fyfe, C. A.; Gobbi, G. C.; Kennedy, G. J. *J. Phys. Chem.* **1985**, *89*, 277–281.
(28) Lowen, W. K.; Broge, E. C. *J. Phys. Chem.* **1961**, *65*, 16–19.
(29) Iler, R. K. *The Chemistry of Silica*; John Wiley & Sons: New York, 1979; p 636.
(30) Zhuravlev, L. T. *Langmuir* **1987**, *3*, 316–318.

and should be studied in detail.

In practice, as f_g is constant in the domain studied (for n_{OH} values ranged between 5 and 15 OH/nm^2), the measure of f_s using only one ^{1}H DEC/MAS spectrum allows the determination of the concentration of hydroxyl groups in the sample. Therefore, we define a simple, routine experiment to characterize an amorphous silica.

The fact that the number of surface hydroxyl groups is greater than the theorical value calculated on such surfaces implies that there is an internal surface only accessible to water molecules the size of which must be about the same as one of the external surface accessible to nitrogen or krypton molecules.

Registry No. Silica, 7631-86-9.

Solvent Effects on Electron Delocalization in Paramagnetic Organometallic Complexes: Solvent Manipulation of the Amount of 19-Electron Character in $Co(CO)_3L_2$ (L_2 = a Chelating Phosphine)

Fei Mao,[1] David R. Tyler,*[,1] Mitchell R. M. Bruce,*[,2] Alice E. Bruce,[2] Anne L. Rieger,[3] and Philip H. Rieger*[,3]

Contribution from the Departments of Chemistry, University of Oregon, Eugene, Oregon 97403, University of Maine, Orono, Maine 04469, and Brown University, Providence, Rhode Island 02912. *Received February 19, 1992*

Abstract: Infrared, ESR, and electronic absorption spectroscopic studies are reported on the 18+δ $Co(CO)_3L_2$ complex. (L_2 is the chelating phosphine ligand 2,3-bis(diphenylphosphino)maleic anhydride. 18+δ complexes are "19-electron complexes" in which the unpaired electron is primarily localized on a ligand.) The spectra are solvent dependent and are interpreted in terms of increased delocalization of the unpaired electron from an $L_2(\pi^*)$ orbital onto the $Co(CO)_3$ portion of the molecule with decreasing solvent polarity. The relationship between the extent of delocalization onto the $Co(CO)_3$ and the substitution reactivity of the molecule was studied. Increased delocalization increases the rate of CO loss (and hence dissociatively activated substitution) because the acceptor molecular orbital on the $Co(CO)_3$ fragment is Co–CO antibonding (k(benzene,25°) = (7.46 ± 0.04) × 10^{-2} s^{-1}; $k(CH_2Cl_2,25°)$ = (5.47 ± 0.03) × 10^{-3} s^{-1}). These substitution results are an exception to the rule of thumb which states that the lability of M–CO bonds decreases as the ν(C≡O) frequencies decrease. An SCF-Xα-SW calculation on the $Co(CO)_3L_2'$ complex (L_2' = 2,3-bis(phosphino)maleic anhydride; i.e. L_2' is L_2 with the phenyl groups replaced by H atoms) confirmed previous ESR spectroscopic results which showed that the SOMO on the $Co(CO)_3L_2$ complex is primarily an L_2-based π^* orbital.

Introduction

Our laboratory is investigating the chemical, physical, and spectroscopic properties of 19-electron organometallic adducts.[4-6] These complexes are formed by the reaction of 17-electron organometallic radicals with 2-electron-donor ligands:[4-17]

$$\underset{17e^-}{ML_n} + L' \overset{K_{eq}}{\rightleftharpoons} \underset{19e^-}{ML_nL'} \qquad (1)$$

ML_n =
$CpMo(CO)_3$, $CpW(CO)_3$, $CpFe(CO)_2$, $Mn(CO)_5$, $Co(CO)_4$

L′ = PR_3, $P(OR)_3$, NR_3, halides, pseudohalides, oxygen atom donors, CH_3CN, THF, and other coordinating solvents

The 19-electron adducts are reactive species, generally forming only as short-lived intermediates in radical reactions.[5-7,18]

Our strategy for stabilizing the 19-electron complexes, so as to make them more amenable to study, is to introduce a ligand with a low-energy π^* orbital into the complex.[4-6,10,19,20] Comparison of parts a and b of Figure 1 shows that if the ligand π^* orbital is sufficiently low in energy then the unpaired electron will

(1) University of Oregon.
(2) University of Maine.
(3) Brown University.
(4) Tyler, D. R. In *Organometallic Radical Processes*; Trogler, W. C., Ed.; Elsevier: New York, 1990; pp 338-364.
(5) Stiegman, A. E.; Tyler, D. R. *Comments Inorg. Chem.* **1986**, *5*, 215-245.
(6) Mao, F.; Philbin, C. E.; Weakley, T. J. R.; Tyler, D. R. *Organometallics* **1990**, *9*, 1510-1516.
(7) The adducts that form in the reactions of 17-electron species with ligands are known in the literature as "19-electron adducts" (or "19-electron complexes") simply because the sun of 17 valence electrons from the metal radical and 2 electrons from the ligand is 19. No implication about the electronic or geometric structures of these complexes is necessarily implied by this name. "Slipped" Cp rings, bent CO ligands (i.e., CO acting as a 1-electron donor), and phosphoranyl radical-type structures are all possible and would result in an 18- or 17-electron configuration at the metal center.
(8) Goldman, A. S.; Tyler, D. R. *Inorg. Chem.* **1987**, *26*, 253-258.
(9) Stiegman, A. E.; Tyler, D. R. *Coord. Chem. Rev.* **1985**, *63*, 217-240.
(10) Tyler, D. R.; Mao, F. *Coord. Chem. Rev.* **1990**, *97*, 119-140.
(11) (a) Fox, A.; Malito, J.; Poë, A. *J. Chem. Soc., Chem. Commun.* **1981**, 1052-1053. (b) Fawcett, J. P.; Jackson, R. A.; Poë, A. *J. Chem. Soc., Chem. Commun.* **1975**, 733-734.
(12) (a) Shi, Q.; Richmond, T. G.; Trogler, W. C.; Basolo, F. *J. Am. Chem. Soc.* **1982**, *104*, 4032-4034. (b) Trogler, W. C. *Int. J. Chem. Kinet.* **1987**, *19*, 1025-1047.
(13) Hershberger, J. W.; Klinger, R. J.; Kochi, J. *J. Am. Chem. Soc.* **1983**, *105*, 61-73.
(14) (a) Kidd, D. R.; Cheng, C. P.; Brown, T. L. *J. Am. Chem. Soc.* **1978**, *100*, 4103-4107. (b) McCullen, S. B.; Brown, T. L. *J. Am. Chem. Soc.* **1982**, *104*, 7496-7500. (c) Walker, H. W.; Rottinger, G. B.; Belford, R. L.; Brown, T. L. *Organometallics* **1983**, *2*, 775-776.
(15) It is interesting to note that K_{eq} has been measured for several of the reactions in which 19-electron adducts form. The formation of the 19-electron adduct is frequently thermodynamically downhill. See: Philbin, C. E.; Granatir, C. A.; Tyler, D. R. *Inorg. Chem.* **1986**, *25*, 4806. See also refs 16 and 17.
(16) Trogler, W. C.; Therien, M. J. *J. Am. Chem. Soc.* **1987**, *109*, 5127-5133.
(17) Kuchynka, D. J.; Kochi, J. K. *Inorg. Chem.* **1988**, *27*, 2574-2581.
(18) Typically, the reactivity of 19-electron complexes consists of either electron transfer to form a stable 18-electron complex or loss of a ligand to form a 17-electron species.[5-7]
(19) Mao, F.; Tyler, D. R.; Keszler, D. *J. Am. Chem. Soc.* **1989**, *111*, 130-134.
(20) Mao, F. Ph.D. Thesis, University of Oregon, 1990.

0002-7863/92/1514-6418$03.00/0